ANALYSIS FOR LEAKAGE AND ROTORDYNAMIC COEFFICIENTS OF SURFACE ROUGHENED TAPERED ANNULAR GAS SEALS*

C. C. Nelson
Texas A&M University
College Station, Texas 77843

ABSTRACT

In order to soften the effects of rub, the smooth stators of turbine gas seals are sometimes replaced by a honeycomb surface. This deliberately roughened stator and smooth rotor combination retards the seal leakage and may lead to enhanced rotor stability. However, many factors determine the rotordynamic coefficients and little is known as to the effectiveness of these "honeycomb seals" under various changes in the independent seal parameters. This analysis develops an analytical-computational method to solve for the rotordynamic coefficients of this type of compressible-flow seal.

The governing equations for surface roughened tapered annular gas seals are based on a modified Hirs' turbulent bulk flow model. A perturbation analysis is employed to develop zeroth and first-order perturbation equations. These equations are numerically integrated to solve for the leakage, pressure, density, and velocity for small motion of the shaft about the centered position. The resulting pressure distribution is then integrated to find the corresponding rotordynamic coefficients. Finally, an example case is used to demonstrate the effect of changing from a smooth to a rough stator while varying the seal length, taper, preswirl, and clearance ratio.

NOMENCLATURE

$C(Z)$	= Centered position seal clearance
$\bar{C} = (C_e+C_x)/2$	= Nominal seal clearance
$\bar{c} = \bar{C}/R$	= Dimensionless nominal seal clearance
c_v	= Specific heat at constant volume
C, c	= Direct and cross-coupled damping coefficients of Eq. (1)
$\tilde{C}$, $\tilde{c}$	= Dimensionless direct and cross-coupled damping coefficients defined by Eq. (26)
D	= Shaft diameter
$H(Z,\theta,t)$	= Local seal clearance
$h = H/\bar{C}$	= Dimensionless clearance
k	= Entrance loss coefficient
K, k	= Direct and cross-coupled stiffness coefficients of Eq. (1)
$\tilde{K}$, $\tilde{k}$	= Dimensionless direct and cross-coupled stiffness coefficients defined by Eq. (25)
L	= Seal length
$\ell = L/R$	= Dimensionless seal length
$M = U_z\sqrt{\frac{\rho}{\gamma p}}$	= Mach number
m_s, m_r, n_s, n_r	= Coefficients for Hirs' turbulent lubrication equations
$P_c = \frac{p_a}{(R\omega)^2\rho_a}$	= Pressure coefficient
p	= Pressure
$\tilde{p} = p/p_a$	= Dimensionless pressure
R	= Shaft radius
$R_{ao} = \frac{2\rho U_z C}{\mu}$	= Centered position, axial Reynolds number
$R_c = \rho(R\omega)\bar{H}/\mu$	= Circumferential Reynolds Number
$R_{co} = \rho(R\omega)\bar{C}/\mu$	= Centered position, nominal circumferential Reynolds number
R_g	= Perfect gas constant
T	= Temperature
t	= Time

*This work is being supported by NASA Grant NAG3-181 from the Lewis Research Center.

$U = R\omega$	= Velocity of rotor surface
U_z, U_θ	= Fluid velocity in the z and θ directions
$u_\theta = U_\theta/(R\omega)$ $u_z = U_z/(R\omega)$	= Dimensionless tangential and axial velocities
Z, Rθ	= Axial and circumferential seal coordinates illustrated in Fig. (1)
$z = Z/L$, θ	= Dimensionless seal coordinates
$\gamma = c_p/c_v$	= Specific heat ratio
ε	= Dimensionless seal eccentricity ratio
$e/2\bar{C}$	= Relative surface roughness
μ	= Viscosity
ρ	= Density
$\tilde{\rho} = \rho/\rho_a$	= Dimensionless density
τ_s, τ_r	= Shear stress illustrated in Fig. (2)
$\tau = \tau\omega$	= Dimensionless time
Ω	= Shaft orbital velocity
$\tilde{\Omega} = \Omega/\omega$	= Shaft whirl ratio
ω	= Shaft angular velocity

Subscripts:

a, e, x, b	= Reservoir, entrance, exit, and sump conditions, respectively
0, 1	= Zeroth and first-order perturbations in the dependent variables
s, r	= Stator surface and rotor surface, respectively

INTRODUCTION

Figure 1 illustrates the basic geometry of the convergent tapered annular turbine gas seal. In this figure both the rotor and the stator elements of the seal are shown to have the same nominally smooth surfaces. In practice, however, the smooth stator is sometimes replaced by a honey comb or other deliberately roughened surface. The purpose of this roughened surface is to soften the effects of rub from the rotor and to retard leakage. But in addition, the smooth rotor and rough stator combination may have significant influence on the seal's rotordynamic coefficients. In fact, von Pragenau [1] suggests just such a concept for an incompressible-flow "damper seal" which he believes will enhance rotor stability.

As related to rotordynamics, seal analysis has the objective of determining the reaction force acting on the rotor as a result of the shaft motion. For small motion about a centered position, the relation between the reaction-force components and the shaft motion can be written

$$-\begin{Bmatrix} F_X \\ F_Y \end{Bmatrix} = \begin{bmatrix} K & k \\ -k & K \end{bmatrix} \begin{Bmatrix} X \\ Y \end{Bmatrix} + \begin{bmatrix} C & c \\ -c & C \end{bmatrix} \begin{Bmatrix} \dot{X} \\ \dot{Y} \end{Bmatrix} + \begin{bmatrix} M & m \\ -m & M \end{bmatrix} \begin{Bmatrix} \ddot{X} \\ \ddot{Y} \end{Bmatrix} \quad (1)$$

The off-diagonal coefficients (k, c, m) are referred to as the cross-coupled stiffness, damping, and added-mass terms, respectively. These cross-coupled terms arise from the fluid's circumferential velocity component. This phenomenon is usually referred to as the effects of swirl. The circumferential velocity component is in part a function of the stator and rotor surface roughness. A rough stator and smooth rotor will tend to reduce the circumferential velocity, leading to a reduction in the destabilizing cross-coupled terms.

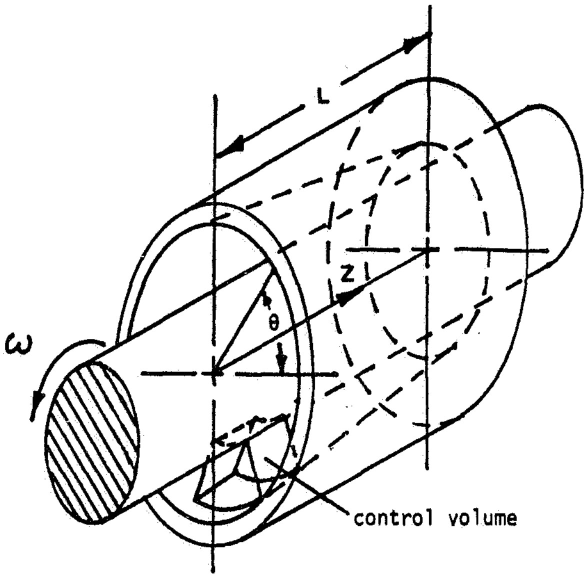

Figure 1. Smooth Tapered Annular Seal.

Fleming [2,3] made a separate analysis for the direct stiffness K, and for the direct damping C of smooth tapered annular gas seals. However, he did not include the effects of swirl and thus could not obtain the cross-coupled terms. Childs [4] developed an analysis for both direct and cross-coupled terms of incompressible-flow by using Hirs' [5] turbulent bulk-flow model and a perturbation technique. Nelson [6] used a similar approach to develop a numerical solution for the direct and cross-coupled stiffness and damping of smooth compressible-flow seals. The present analysis modifies the solution of reference [6] to include the effects of different stator and rotor surface conditions and then demonstrates the analysis on a specific seal example.

GOVERNING EQUATIONS

The control volume element shown in Fig. 1 has been enlarged and redrawn in Fig. 2. Note that the smooth stator surface has been replaced by a roughened honeycomb surface. The shear stresses τ_s and τ_r are the net wall shear stresses resulting from both the pressure induced flow and the drag induced flow. Hirs' turbulent bulk-flow model assumes that these stresses can be written as

$$\tau = \tfrac{1}{2}\rho U_m^2 n_o \left(\frac{2\,U_m H}{\mu}\right)^{m_o} \quad (2)$$

where U_m is the mean flow velocity relative to the surface upon which the shear stress is acting. Hirs' constants n_o and m_o are generally empirically determined from pressure flow experiments. For the control

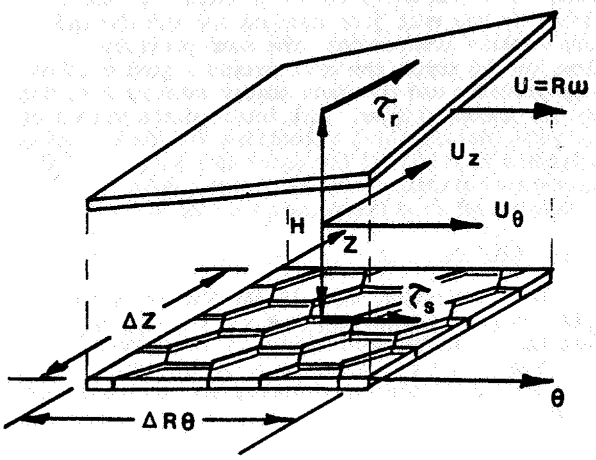

Figure 2. Control Volume for a Seal with a Honeycomb Stator.

volume in Fig. 2, n_s and m_s represent Hirs' constants relative to the stator surface and n_r and m_r represent those relative to the rotor surface. Substituting the mean flow velocity relative to each surface into Eq. (2) and then taking the appropriate component of the shear stress in the Z and θ-direction, the axial and circumferential momentum equations are

$$-H\frac{\partial p}{\partial Z} = \rho\left\{\frac{n_s}{2}\left(\frac{2\rho H}{\mu}\right)^{m_s} U_z\left(U_\theta^2+U_z^2\right)^{\frac{m_2+1}{2}} + \frac{n_r}{2}\left(\frac{2\rho H}{\mu}\right)^{m_r} U_z\left[(U_\theta-U)^2+U_z^2\right]^{\frac{m_r+1}{2}}\right\} + \frac{\partial(\rho U_\theta H)}{\partial t} + \frac{1}{R}\frac{\partial(\rho U_\theta U_z H)}{\partial\theta} + \frac{\partial(\rho U_z^2 H)}{\partial Z} \quad (3a)$$

$$-\frac{H}{R}\frac{\partial p}{\partial\theta} = \rho\left\{\frac{n_s}{2}\left(\frac{2\rho H}{\mu}\right)^{m_s} U_\theta\left(U_\theta^2+U_z^2\right)^{\frac{m_s+1}{2}} + \frac{n_r}{2}\left(\frac{2\rho H}{\mu}\right)^{m_r}(U_\theta-U)\left[(U_\theta-U)^2+U_z^2\right]^{\frac{m_r+1}{2}}\right\} + \frac{\partial(\rho U_\theta H)}{\partial t} + \frac{1}{R}\frac{\partial(\rho U_\theta^2 H)}{\partial\theta} + \frac{\partial(\rho U_\theta U_z H)}{\partial Z} \quad (3b)$$

The bulk-flow continuity equation is

$$0 = \frac{\partial(\rho H)}{\partial t} + \frac{1}{R}\frac{\partial(\rho U_\theta H)}{\partial\theta} + \frac{\partial(\rho U_z H)}{\partial Z} \quad (3c)$$

And for adiabatic flow the energy equation is

$$0 = \frac{\partial}{\partial t}\left[\left(c_vT+\frac{U_\theta^2}{2}+\frac{U_z^2}{2}\right)\rho H\right] + \frac{1}{R}\frac{\partial}{\partial\theta}\left[\left(c_vT+\frac{U_\theta^2}{2}+\frac{U_z^2}{2}+\frac{p}{\rho}\right)U_\theta\rho H\right] + \frac{\partial}{\partial Z}\left[\left(c_vT+\frac{U_\theta^2}{2}+\frac{U_z^2}{2}+\frac{p}{\rho}\right)U_z\rho H\right] + U(U_\theta-U)\frac{\rho n_r}{2}\left(\frac{2\rho H}{\mu}\right)^{m_r}\left[(U_\theta-U)^2+U_z\right]^{\frac{m_r+1}{2}} \quad (3d)$$

Assuming a perfect gas ($c_vT=p/\rho(\gamma-1)$) and using the dimensionless parameters defined in the Nomenclature, the above governing equations take the following dimensionless working form.

Momentum:

$$\frac{-P_c}{\tilde{\rho}\ell}\frac{\partial\tilde{p}}{\partial z} = \frac{u_z}{ch}\left[f_s+f_r\right] + \frac{Du_z}{D\tau} \quad (4a)$$

$$\frac{-P_c}{\tilde{\rho}}\frac{\partial\tilde{p}}{\partial\theta} = \frac{1}{ch}\left[u_\theta f_s + (u_\theta-1)f_r\right] + \frac{Du_\theta}{D\tau} \quad (4b)$$

Continuity:

$$0 = \frac{\partial(\tilde{\rho}h)}{\partial\tau} + \frac{\partial(\tilde{\rho}u_\theta h)}{\partial\theta} + \frac{1}{\ell}\frac{\partial(\tilde{\rho}u_z h)}{\partial z} \quad (4c)$$

Energy:

$$\frac{\tilde{p}}{h}\frac{\partial h}{\partial\tau} = u_\theta\left(\frac{\partial\tilde{p}}{\partial\theta}+\frac{\tilde{\rho}}{P_c}\frac{Du_\theta}{D\tau}\right) + u_z\left(\frac{1}{\ell}\frac{\partial\tilde{p}}{\partial z}+\frac{\tilde{\rho}}{P_c}\frac{Du_z}{D\tau}\right) + \frac{1}{\gamma-1}\left(\frac{D\tilde{p}}{D\tau}-\frac{\gamma\tilde{p}}{\tilde{\rho}}\frac{D\tilde{\rho}}{D\tau}\right) + \frac{\tilde{\rho}}{chP_c}(u_\theta-1)f_r \quad (4d)$$

where

$$f_s = \frac{n_s}{2}\left(u_\theta^2+u_z^2\right)^{\frac{m_s+1}{2}}(2R_c)^{m_s}$$

$$f_r = \frac{n_r}{2}\left[(u_\theta-1)^2+u_z^2\right]^{\frac{m_r+1}{2}}(2Rc)^{m_r} \quad (4e)$$

$$\frac{D}{D\tau} = \frac{\partial}{\partial\tau} + u_\theta\frac{\partial}{\partial\theta} + \frac{u_z}{\ell}\frac{\partial}{\partial z}$$

PERTURBATION ANALYSIS

The governing Eqs. (4a) through (4d) define the relationship between the dimensionless clearance, pressure, density, axial velocity, and circumferential velocity (h, $\tilde{p}$, $\tilde{\rho}$, u_z, u_θ) as functions of the independent dimensionless spatial variables (θ, z) and the dimensionless time τ. Expansion of these equations in the perturbation variables

$$h = h_o + \varepsilon h_1 \quad \tilde{\rho} = \tilde{\rho}_o + \varepsilon\tilde{\rho}_1 \quad u_\theta = u_{\theta o} + \varepsilon u_{\theta 1}$$

$$\tilde{p} = \tilde{p}_o + \varepsilon\tilde{p}_1 \quad u_z = u_{zo} + \varepsilon u_{z1} \quad (5)$$

yields the zeroth and first-order equations as shown in Appendix A.

Zeroth-Order Solution

The zeroth-order equations describe the steady flow resulting from a centered position rotating shaft. Before these equations can be integrated, values for Hirs' constants m_s, n_s, m_r, and n_r must be established. Lacking experimental data for these constants, values can be approximated by the use of Colebrook's formula [7].

$$\frac{1}{\sqrt{4n_o R_a^{mo}}} = -2 \log \left(\frac{e/2\bar{C}}{3.7} + \frac{2.51}{R_a\sqrt{4n_o R_a^{mo}}} \right) \qquad (6)$$

For a given relative roughness a least-squares fit is used to determine n_o and m_o over a range of R_a (say $5000<R_a<1000000$).

Integration begins by guessing an entrance zeroth-order Mach number $M_o(0)$. Defining an entrance loss coefficient k in a manner similar to Zuk [8], the following equations give the initial zeroth-order pressure and density.

$$\tilde{p}_o(0) = \frac{1}{\left[1 + \frac{(\gamma-1)(1+k)M_o^2(0)}{2}\right]^{\gamma/(\gamma-1)}} \qquad (7)$$

$$\tilde{\rho}_o(0) = \frac{1 + \left[\frac{(\gamma-1)M_o^2(0)}{2}\right]}{\left[1 + \frac{(\gamma-1)(1+k)M_o^2(0)}{2}\right]^{\gamma/(\gamma-1)}} \qquad (8)$$

In the first application, k is assumed to be 0.1. Expanding the Mach number as defined in the nomenclature in terms of the perturbation variables gives the following zeroth-order entrance equation

$$M_o^2(0) = \frac{u_{zo}^2(0)\tilde{\rho}_o(0)}{\gamma\tilde{p}_o(0)P_c} \qquad (9)$$

From this equation, the initial zeroth-order axial velocity $u_{zo}(0)$ can be found. Having now $\tilde{p}_o(0)$, $\tilde{\rho}_o(0)$, and $u_{zo}(0)$, the centered position axial Reynolds number R_{ao} is determined and used to approximate a new loss coefficient from the data of Deissler [9] as

$$k = \sqrt{5.3/\log_{10}R_{ao}} - 1.0 \qquad (10)$$

For $R_{ao}>200{,}000$, k is set equal to zero. This new loss coefficient is then used to determine new entrance conditions and the procedure repeated until a consistent result for k is found. Finally, the initial zeroth-order circumferential velocity, $u_\theta(0)$, is a given independent variable which indicates the amount of prerotation given to the entering fluid.

Having now the zeroth-order initial conditions, Eqs. (A.1a) through (A.1d) are numerically integrated along the seal length. The guess for the entrance Mach number is continually adjusted until: (a) the Mach number at the exit just reaches one and the exit pressure remains greater than the sump pressure for choked flow, or (b) until the exit pressure just matches the sump pressure and the Mach number remains less than one for unchoked flow. All intermediate values of the pressure, density, and velocities and their derivatives are then stored for later use in solving the first-order perturbation equations. Also, the leakage is determined from these zeroth-order values.

First-Order Solution

The first-order Eqs. (A.2a) through (A.2d) define $\tilde{p}_1(z,\theta,\tau)$, $\tilde{\rho}_1(z,\theta,\tau)$, $u_{z1}(z,\theta,\tau)$, and $u_{\theta 1}(z,\theta,\tau)$ resulting from the seal clearance function $h_1(z,\theta,\tau)$. If the shaft center moves in an elliptical orbit, then the rotation displacement vector to the shaft center has coordinates

$$X = Cx_o\cos\Omega t \quad , \quad Y = Cy_o\sin\Omega t \qquad (11)$$

and the clearance function is

$$h_1 = -x_o\cos\tilde{\Omega}\tau\cos\theta - y_o\sin\tilde{\Omega}\tau\sin\theta \qquad (12)$$

The assumed harmonic response is

$$\begin{aligned}
\tilde{p}_1 &= (\tilde{p}_x^c\cos\tilde{\Omega}\tau+\tilde{p}_x^s\sin\tilde{\Omega}\tau)\cos\theta+(\tilde{p}_y^c\cos\tilde{\Omega}\tau+\tilde{p}_y^s\sin\tilde{\Omega}\tau)\sin\theta \\
\tilde{\rho}_1 &= (\tilde{\rho}_x^c\cos\tilde{\Omega}\tau+\tilde{\rho}_x^s\sin\tilde{\Omega}\tau)\cos\theta+(\tilde{\rho}_y^c\cos\tilde{\Omega}\tau+\tilde{\rho}_y^s\sin\tilde{\Omega}\tau)\sin\theta \\
u_{z1} &= (u_x^c\cos\tilde{\Omega}\tau+u_x^s\sin\tilde{\Omega}\tau)\cos\theta+(u_y^c\cos\tilde{\Omega}\tau+u_y^s\sin\tilde{\Omega}\tau)\sin\theta \\
u_{\theta 1} &= (v_x^c\cos\Omega\tau+v_x^s\sin\Omega\tau)\cos\theta+(v_y^c\cos\Omega\tau+v_y^s\sin\Omega\tau)\sin\theta
\end{aligned} \qquad (13)$$

Substitution of Eqs. (12) and (13) into the first-order Eqs. (A.2a) through (A.2d) yields sixteen first-order ordinary differential equations which can be written in the form

$$[A(z)]\frac{d\underline{X}}{dz} + [B(z)]\underline{X} = x_o\underline{C}(z) + y_o\underline{D}(z) \qquad (14)$$

where

$$\underline{X}=(\tilde{p}_x^c,\tilde{p}_x^s,\tilde{p}_y^c,\tilde{p}_y^s,\tilde{\rho}_x^c,\tilde{\rho}_x^s,\tilde{\rho}_y^c,\tilde{\rho}_y^s,u_x^c,u_x^s,u_y^c,u_y^s,v_x^c,v_x^s,v_y^c,v_y^s).$$

The coefficients of [A], [B], $\underline{C}$, and $\underline{D}$ are given in Appendix B. These coefficients are completely determined from the values obtained in the zeroth-order solution.

The necessary sixteen boundary conditions for Eq. (14) are now written by examining the perturbation conditions that must exist at the entrance and exit for choked or unchoked flow. For ease in writing these conditions, the following definitions are made:

$$\underline{p}_1 = \begin{Bmatrix} \tilde{p}_x^c \\ \tilde{p}_x^s \\ \tilde{p}_y^c \\ \tilde{p}_y^s \end{Bmatrix}, \quad \underline{\rho}_1 = \begin{Bmatrix} \tilde{\rho}_x^c \\ \tilde{\rho}_x^s \\ \tilde{\rho}_y^c \\ \tilde{\rho}_y^s \end{Bmatrix}, \quad \underline{u}_{z1} = \begin{Bmatrix} u_x^c \\ u_x^s \\ u_y^c \\ u_y^s \end{Bmatrix}, \quad \underline{u}_{\theta 1} = \begin{Bmatrix} v_x^c \\ v_x^s \\ v_y^c \\ v_y^s \end{Bmatrix} \qquad (15)$$

(a.1) For choked flow, the first-order perturbation in in the exit Mach number is set equal to zero. Using the definition of the Mach number, the first-order perturbation is

$$M_1 = M_o\left(\frac{\tilde{p}_1}{2\tilde{p}_o} + \frac{u_{z1}}{u_{zo}} - \frac{\tilde{\rho}_1}{2\tilde{\rho}_o}\right) \quad (16)$$

This yields

$$\frac{\tilde{p}_1(1)}{2\tilde{p}_o(1)} + \frac{u_{z1}(1)}{u_{zo}(1)} - \frac{\tilde{\rho}_1(1)}{2\tilde{\rho}_o(1)} = 0 \quad (17)$$

(a.2) For unchoked flow, the first-order perturbation in the exit pressure is zero giving

$$\tilde{p}_1(1) = 0 \quad (18)$$

(b) At the entrance, the circumferential velocity perturbation is zero, i.e.

$$u_{\theta 1}(0) = 0 \quad (19)$$

(c) Expansion of the pressure loss Eq. (7) in terms of the perturbation pressure and the perturbation Mach number from Eq. (16) yields the following first-order pressure loss equation which must be satisfied at the entrance:

$$\tilde{p}_1(0) + \frac{r\tilde{p}_o(0)}{2\tilde{p}_o(0)-r}\left(\frac{\tilde{\rho}_1(0)}{\tilde{\rho}_o(0)} + \frac{2u_{z1}(0)}{u_{zo}(0)}\right) = 0 \quad (20)$$

where

$$r = \frac{\gamma(k+1)\tilde{p}_o(0)M_o^2(0)}{1+(\gamma-1)(k+1)\dfrac{M_o^2(0)}{2}} \quad (21)$$

(d) A similar expansion for the density change at the entrance defined by Eq. (8) gives

$$\tilde{\rho}_1(0) + \frac{rs\tilde{\rho}_o(0)}{2\tilde{p}_o(0)+rs}\left(\frac{2u_{z1}(0)}{u_{zo}(0)} - \frac{\tilde{p}_1(0)}{\tilde{p}_o(0)}\right) = 0 \quad (22)$$

where

$$s = 1+(\gamma-1)\frac{[M_o^2(0)(k+1)-2]}{2\gamma(k+1)} \quad (23)$$

Solution of the differential Eq. (14) in terms of the above sixteen boundary conditions can be found by numerical integration techniques. The solution will take the form

$$\underline{X} = x_o\underline{f}(z) + y_o\underline{g}(z) \quad (24)$$

Dynamic Coefficient Definitions

As shown in reference [6] if the added mass terms are neglected, the dynamic seal coefficients can be obtained by numerically integrating the appropriate solution component of Eq. (24), i.e.,

$$\tilde{K} = \frac{K\bar{C}}{P_aRL} = \pi\int_0^1 f_1(z)dz \quad \tilde{k} = \frac{k\bar{C}}{P_aRL} = -\pi\int_0^1 f_3(z)dz \quad (25)$$

$$\tilde{C} = \frac{C\bar{C}\,\Omega}{P_aRL} = \pi\int_0^1 g_3(z)dz \quad \tilde{c} = \frac{c\bar{C}\Omega}{P_aRL} = \pi\int_0^1 g_1(z)dz \quad (26)$$

NUMERICAL EXAMPLE

For the compressible flow seal with different stator-rotor surface roughness treatments, there are fourteen independent geometric and fluid dynamic seal variables. Assuming a perfect gas, these variables can be reduced to ten dimensionless parameters. One possible set is $P_c=p_a/(\rho_a\omega^2R^2)$, $R_{coa}=\rho_a\bar{C}\omega R/\mu$, p_a/p_b, γ, L/D, C_e/C_x, $\bar{C}/R$, $e_s/2\bar{C}$, $e_r/2\bar{C}$ and $u_\theta(0)=U_\theta(0)/(\omega R)$. Due to this large number of independent parameters, it is unreasonable to attempt to describe the leakage and dynamic coefficient's dependence in the form of a complete set of design charts. Thus, a specific seal geometry and flow condition was chosen, and only the length, taper, fluid prerotation, and clearance ratio (L/D, C_e/C_x, $u_{\theta o}(0)$, and $\bar{C}/R$) were independently varied. The particular seal selected is equivalent to the turbine interstage seal of the High Pressure Oxidizer Turbopump (HPOTP) of the Space Shuttle Main Engine operating at Rated Power Level. The rotor is smooth and the stator is a honeycomb surface, resulting in the following seal parameters as supplied by Jackson [10]:

p_a = 34.05 MPa (4938 psia)

p_b = 26.41 MPa (3830 psia)

T_a = 773°K (1391°R)

R = 7.282 cm (2.867 in)

C_e = 0.381 mm (0.015 in)

C_x = 0.254 mm (0.010 in)

L = 2.527 cm (0.995 in)

γ = 1.4

R_g = 2480 m·N/kg°K (461 ft·lb/lbm°R)

$\mu = 2.05 \times 10^{-5}$ Pa·s (1.38×10^{-5} lb_m/ft·s)

$U_{\theta o}(0)$ = 0.25

ω = 28352 rpm

$e_s/2\bar{C} = 1.54 \times 10^{-2} \Rightarrow m_s = -0.0251$, $n_s=0.01534$

$e_r/2\bar{C} = 3.08 \times 10^{-4} \Rightarrow m_r = -0.1691$, $n_r=0.03976$

Results obtained for this seal are shown in Table 1. The first row of data represents the seal with the given smooth rotor and rough stator. The second row represents the results if both the stator and rotor are smooth. As expected, the rough stator decreases the leakage and cross-coupled stiffness. However, it also has the effect of significantly reducing the direct stiffness and slightly decreasing the direct damping.

	$\dot{\rho}$ (kg/s)	$K\times10^{-7}$ (N/m)	$k\times10^{-7}$ (N/m)	C (N·s/m)	c (N·s/m)
rough	1.23	3.07	0.147	1770	13.0
smooth	1.35	3.40	0.160	1800	-0.9

Table 1. Leakage and Rotordynamic Coefficients for the HPOTP Turbine Interstage Seal

Results obtained by varying the seal geometry are plotted in Figs. 3 through 6. In these graphs, the broken lines represent the given rough stator and the continuous lines represent a smooth stator. The

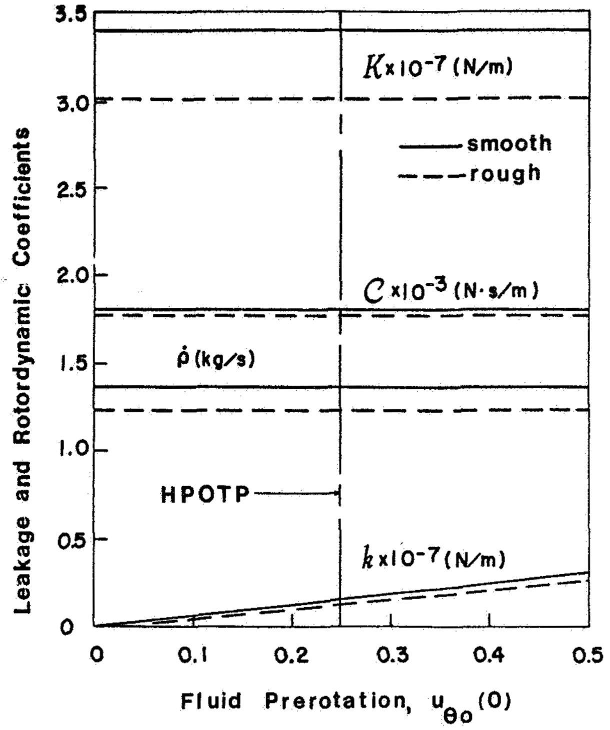

Figure 3. Leakage and rotordynamic coefficients vs. fluid prerotation (unchoked flow)

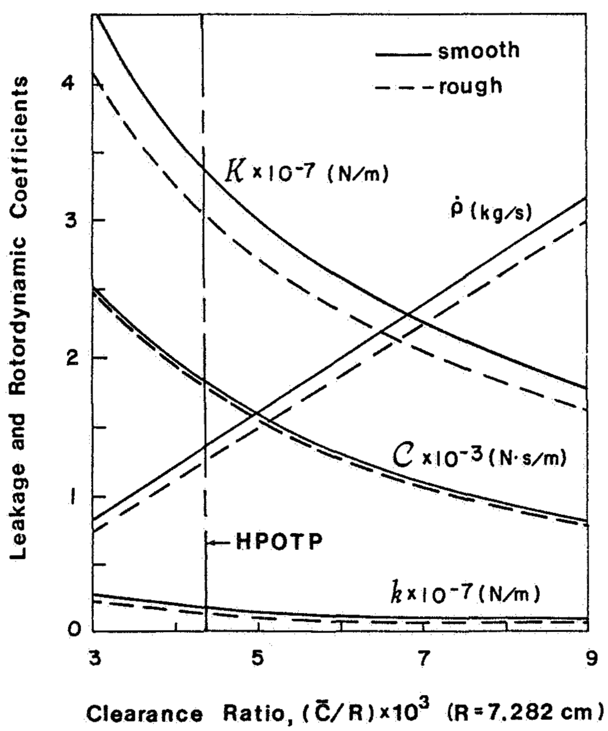

Figure 4. Leakage and Rotordynamic Coefficients vs. Clearance Ratio. (unchoked flow)

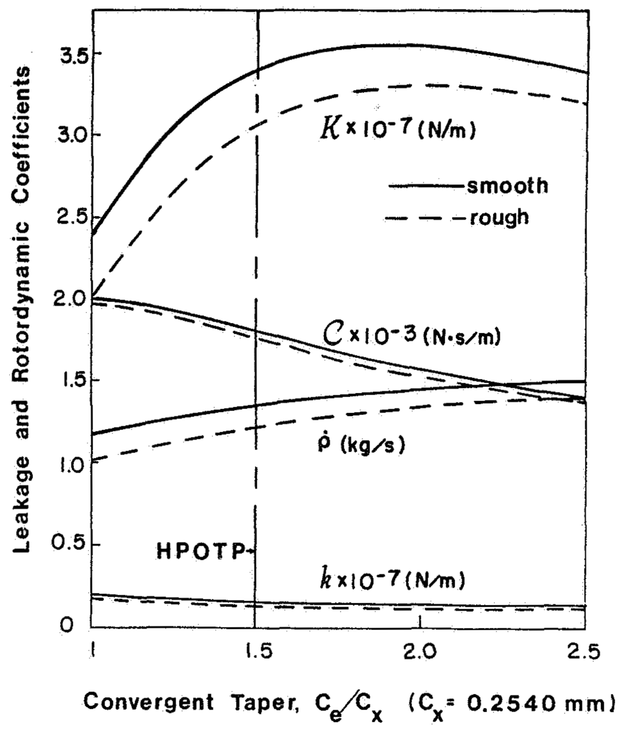

Figure 5. Leakage and Rotordynamic Coefficients vs. Convergent Taper (unchoked flow)

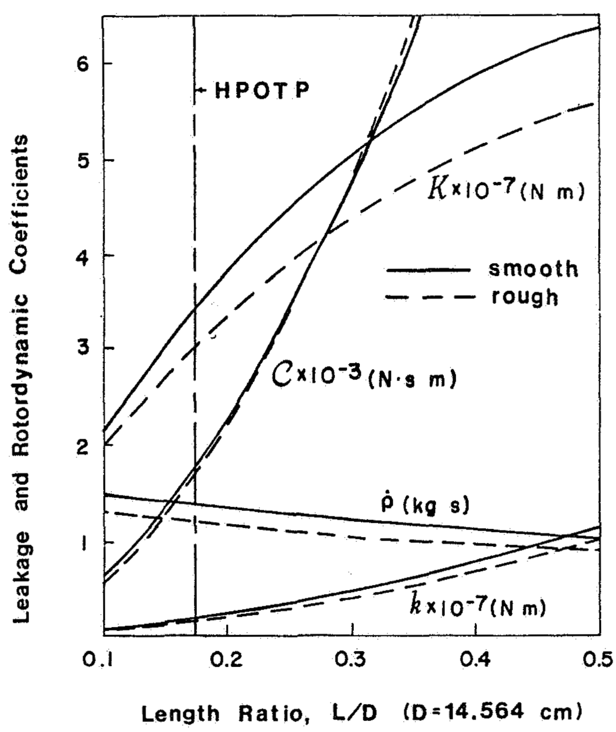

Figure 6. Leakage and rotordynamic coefficients vs. length ratio (unchoked flow)

vertical broken line represents the actual value of the independent variable for the HPOTP seal. Cross-coupled damping is not shown since it was found to be relatively insignificant.

Figure 3 shows the effect of fluid prerotation (preswirl). Clearly, prerotation has no effect on $\tilde{\rho}$, K, or C. However, there is a direct linear relationship for k.

Figure 4 shows the effect of changing the nominal clearance $\bar{C}$ (convergent taper was held constant). Within the range shown, decreasing the clearance results in an exponential increase in all coefficients and a linear decrease in leakage.

Figure 5 shows the effect of convergent taper, C_e/C_x. For these results, the exit clearance was held constant and the entrance clearance increased. It should be noted that this also has the effect of increasing the nominal clearance. Thus $1.0 \leq C_e/C_x \leq 2.5$ results in $0.0035 \leq C/R < 0.0061$. As might be expected from Fig. 4, increasing the taper in this manner increases ρ and decreases k and C. However, K shows roughly a 50% increase when the seal is changed from straight to having a convergent taper ratio of $C_e/C_x=2$.

Finally, Fig. 6 shows the effect of seal length. Generally, as L/D increases, the coefficients increase and the leakage decreases. However, for a very long seal (i.e., L/D = 0.8), K does reach a maximum and thereafter decreases.

CONCLUDING REMARKS

An analysis has been presented which calculates the leakage and rotordynamic coefficients for tapered annular gas seals in which the rotor and stator have different surface roughness treatments. To demonstrate this analysis, the effect of changes in seal length, taper, clearance and fluid prerotation was shown for the HPOTP turbine interstage seal. Generally, changes in the abovementioned seal parameters resulted in major changes in the leakage and rotordynamic coefficients.

In terms of the honey comb stator enhancing rotor stability, the results appear mixed. There is a favorable 9% reduction in cross-coupled stiffness and leakage. But at the same time, direct damping decreases almost 2% and direct stiffness decreases 10%. Thus, general statements concerning the problems of instability and critical speeds can only be addressed by considering the entire rotordynamic system - clearly a problem outside the scope of this analysis. It should also be kept in mind that the selection of Hirs' constants may not accurately reflect the actual shear stresses developed over the honey comb surface. Experimental tests need yet to be performed to determine the correct values for these constants.

REFERENCES

1. von Pragenau, G. L., "Damping Seals for Turbomachinery," NASA Technical Paper-1987, George C. Marshall Space Flight Center, Alabama 35812.
2. Fleming, D. P., "Stiffness of Straight and Tapered Annular Gas Path Seals," J. Lubr. Technol., Vol. 101, No. 3, pp. 349-355, July 1979.
3. Fleming, D. P., "Damping in Ring Seals for Compressible Fluids," NASA CP-2133, 1980.
4. Childs, D. W., "Finite Length Solutions for the Rotordynamic Coefficients of Convergent-Turbulent Annular Seals," Mechanical Engineering, Texas A&M University, 1982.
5. Hirs, G. G., "Fundamentals of a Bulk-Flow Theory for Turbulent Lubrication Films," Ph.D. Dissertation, Delft Technical University, The Netherlands, July 1970.
6. Nelson, C. C., "Rotordynamic Coefficients for Compressible Flow in Tapered Annular Seals," Mechanical Engineering, Texas A&M University, 1983.
7. White, F. M., Fluid Mechanics, McGraw-Hill, 1979.
8. Zuk, J., Ludwig, L. P., and Johnson, R. L., "Quasi-One-Dimensional Compressible Flow Across Face Seals and Narrow Slots," NASA Technical Note D-6668, May 1972.
9. Deissler, R. G., "Analysis of Turbulent Heat Transfer and Flow in the Entrance Regions of Smooth Passages," NACA TN 3016, 1953.
10. Jackson, E. D., Manager, Rotating Machinery Analysis, Rockwell International, Rocketdyne Division, personal correspondence, 1983.

APPENDIX A: PERTURBATION EQUATIONS

Zeroth-Order Equations

$$-\frac{P_c}{\tilde{\rho}}\frac{\partial \tilde{p}_o}{\ell\partial z} = \frac{u_{zo}}{\bar{c}h_o}[f_{so}+f_{ro}] + \frac{u_{zo}}{\ell}\frac{\partial u_{zo}}{\partial z} \tag{A.1a}$$

$$0 = \frac{1}{\bar{c}h_o}\left[u_{\theta o}f_{so}+(u_{\theta o}-1)f_{ro}\right] + \frac{u_{zo}}{\ell}\frac{\partial u_{\theta o}}{\partial z} \tag{A.1b}$$

$$0 = \tilde{\rho}_o u_{zo}\frac{\partial h_o}{\partial z} + \tilde{\rho}_o h_o\frac{\partial u_{zo}}{\partial z} + u_{zo}h_o\frac{\partial \tilde{\rho}_o}{\partial z} \tag{A.1c}$$

$$0 = u_{\theta o}\frac{\partial u_{\theta o}}{\partial z} + u_{zo}\frac{\partial u_{zo}}{\partial z} + \frac{P_c\gamma}{\tilde{\rho}_o(\gamma-1)}\left(\frac{\partial p_o}{\partial z} - \frac{p_o}{\tilde{\rho}_o}\frac{\partial \rho_o}{\partial z}\right) + \frac{\ell(u_{\theta o}-1)f_{ro}}{\bar{c}h_o u_{zo}} \tag{A.1d}$$

where

$$f_{so} = \frac{n_s}{2}\left(u_o^2 + u_{zo}^2\right)^{\frac{m_s+1}{2}}(2R_{co})^{m_s}$$

$$f_{ro} = \frac{n_r}{2}\left[(u_o-1)^2 + u_{zo}^2\right]^{\frac{m_r+1}{2}}(2R_{co})^{m_r}$$

First-Order Equations

$$-\frac{P_c}{\tilde{\rho}_o\ell}\frac{\partial \tilde{p}_1}{\partial z} = \frac{-P_c\tilde{\rho}_1}{\tilde{\rho}_o^2\ell}\frac{\partial p_o}{\partial z} + \frac{1}{\bar{c}h_o}\left[u_{zo}(f_{s1}+f_{r1}) + \left(u_{z1}-u_{zo}\frac{h_1}{h_o}\right)(f_{s1}+f_{r1})\right] + \frac{\partial u_{z1}}{\partial \tau} + u_{\theta o}\frac{\partial u_{z1}}{\partial \theta} + \frac{u_{zo}}{\ell}\frac{\partial u_{z1}}{\partial z} + \frac{u_{z1}}{\ell}\frac{\partial u_{zo}}{\partial z} \tag{A.2a}$$

$$\frac{-P_c}{\tilde{\rho}_o}\frac{\partial\tilde{\rho}_1}{\partial\theta} = \frac{1}{\bar{c}h_o}\left[u_{\theta o}\left(f_{s1} - \frac{h_1}{h_o} f_{so}\right)\right.$$

$$+ (u_{\theta o}-1)\left(f_{r1} - \frac{h_1}{h_o} f_{ro}\right) + u_{\theta 1}(f_{so}+f_{ro})$$

$$+ \frac{\partial u_{\theta 1}}{\partial\tau} + u_{\theta o}\frac{\partial u_{\theta 1}}{\partial\tau} + \frac{u_{z0}}{\ell}\frac{\partial u_{\theta 1}}{\partial z} + \frac{u_{z1}}{\ell}\frac{\partial u_{\theta o}}{\partial z} \tag{A.2b}$$

$$0 = \frac{\tilde{\rho}_o}{h_o}\frac{\partial h_1}{\partial\tau} + \frac{\partial\tilde{\rho}_1}{\partial\tau} + \frac{\tilde{\rho}_o u_{\theta o}}{h_o}\frac{\partial h_1}{\partial\theta} + \tilde{\rho}_o\frac{\partial u_{\theta 1}}{\partial\theta} + u_{\theta o}\frac{\partial\tilde{\rho}_1}{\partial\theta}$$

$$+ \frac{1}{\ell h_o}\left[h_1\frac{\partial(\tilde{\rho}_o u_{zo})}{\partial z} + \frac{\partial(\tilde{\rho}_o u_{z1} h_o)}{\partial z} + \frac{\partial(\tilde{\rho}_1 u_{zo} h_o)}{\partial z}\right] \tag{A.2c}$$

$$\frac{P_c\tilde{\rho}_o}{\tilde{\rho}_o h_o}\frac{\partial h_1}{\partial\tau} = u_{zo}\left[\frac{\partial u_{z1}}{\partial\tau} + u_{\theta o}\frac{\partial u_{z1}}{\partial\theta} + \frac{1}{\ell}\left(u_{zo}\frac{\partial u_{z1}}{\partial z}\right.\right.$$

$$\left.\left. + 2u_{z1}\frac{\partial u_{zo}}{\partial z} + u_{\theta 1}\frac{\partial u_{\theta o}}{\partial z}\right)\right] + u_{\theta o}\left[\frac{\partial u_{\theta 1}}{\partial\tau}\right.$$

$$\left. + u_{\theta o}\frac{\partial u_{\theta 1}}{\partial\theta} + \frac{1}{\ell}\left(u_{zo}\frac{\partial u_{\theta 1}}{\partial z} + u_{z1}\frac{\partial u_{\theta o}}{\partial z}\right)\right]$$

$$+ \frac{\gamma P_c}{\tilde{\rho}_o(\gamma-1)}\left\{\frac{1}{\gamma}\frac{\partial\tilde{\rho}_1}{\partial\tau} + u_{\theta o}\frac{\partial\tilde{\rho}_1}{\partial\theta} + \frac{u_{\theta o}}{\ell}\frac{\partial\tilde{\rho}_1}{\partial z}\right.$$

$$+ \frac{1}{\ell}\frac{\partial\tilde{\rho}_o}{\partial z}\left(u_{z1} - u_{zo}\frac{\tilde{\rho}_1}{\rho_o}\right) - \frac{\tilde{\rho}_o}{\rho_o}\left[\frac{\partial\tilde{\rho}_1}{\partial\tau}\right.$$

$$+ u_{\theta o}\frac{\partial\tilde{\rho}_1}{\partial\theta} + \frac{u_{zo}}{\ell}\frac{\partial\tilde{\rho}_1}{\partial z} + \frac{1}{\ell}\frac{\partial\tilde{\rho}_o}{\partial z}\left(u_{z1}\right.$$

$$\left.\left.\left. + u_{zo}\left(\frac{\tilde{\rho}_1}{\tilde{\rho}_o} - \frac{2\tilde{\rho}_1}{\tilde{\rho}_o}\right)\right)\right]\right\}$$

$$+ \frac{\tilde{\rho}_o(u_{\theta o}-1)f_{ro}}{\bar{c}h_o P_c}\left[\frac{\tilde{\rho}_1}{\tilde{\rho}} + \frac{u_{\theta 1}}{(u_{\theta o}-1)} + \frac{f_{r1}}{f_{ro}} - \frac{h_1}{h_o}\right] \tag{A.2d}$$

where

$$f_{s1} = f_{so}\left[m_s\left(\frac{\tilde{\rho}_1}{\tilde{\rho}_o} + \frac{h_1}{h_o}\right) + a(u_{\theta o}u_{\theta 1} + u_{zo}u_{z1})\right.$$

$$f_{r1} = f_{ro}\left[m_r\left(\frac{\tilde{\rho}_1}{\tilde{\rho}_o} + \frac{h_1}{h_o}\right) + b((u_{\theta o}-1)u_{\theta 1} + u_{zo}u_{z1})\right]$$

$$a = (m_s+1)/(u_{\theta o}^2 + u_{zo}^2)$$

$$b = (m_r+1)/[(u_{\theta o}-1)^2 + u_{zo}^2]$$

APPENDIX B: MATRIX COEFFICIENTS

All coefficients are zero except those defined below. Also, $\gamma' = \gamma P_c/[\tilde{\rho}_o(\gamma-1)]$ and $q = \tilde{\rho}_o(u_{\theta o}-1)f_{bo}/(\bar{c}h_o P_c)$

Matrix [A]

$a_{i,i+4} = u_{zo}/\ell$	i=1,2,3...12
$a_{i,i+8} = \tilde{\rho}_o/\ell$	i=1,2,3,4
$a_{i+4,i} = \dfrac{P_c}{\tilde{\rho}_o\ell}$	i=1,2,3,4
$a_{i+12,i} = \gamma' u_{zo}/\ell$	i=1,2,3,4
$a_{i+8,i} = \dfrac{-\gamma'\tilde{\rho}_o u_{zo}}{\tilde{\rho}_o\ell}$	i=5,6,7,8
$a_{i+r,i} = \dfrac{u_{zo}^2}{\ell}$	i=9,10,11,12
$a_{i,i} = \dfrac{u_{zo}u_{\theta o}}{\ell}$	i=13,14,15,16

Matrix [B]

$b_{i,i+4} = \dfrac{1}{\ell h_o}\dfrac{d(u_{zo}h_o)}{dz}$	i=1,2,3,4
$b_{i,i+5} = -b_{i+1,i+4} = \tilde{\Omega}$	i=1,3,5...11
$b_{i,i+6} = -b_{i+2,i+4} = u_{\theta o}$	i=1,2,5,6,9,10
$b_{i,i+8} = \dfrac{1}{\ell h_o}\dfrac{d(\tilde{\rho}_o h_o)}{dz}$	i=1,2,3,4
$b_{i,i+14} = -b_{i+2,i+12} = \tilde{\rho}_o$	i=1,2
$b_{i,i} = \dfrac{u_{zo}}{\bar{c}h_o\tilde{\rho}_o}(m_s f_{so} + m_r f_{ro}) - \dfrac{P_c}{\tilde{\rho}_o^2\ell}\dfrac{d\tilde{\rho}_o}{dz}$	i=5,6,7,8
$b_{i,i+4} = \dfrac{1}{\bar{c}h_o}\left\{f_{so}[1+u_{zo}^2 a] + f_{ro}(1+u_{zo}^2 b)\right\} + \dfrac{1}{\ell}\dfrac{du_{zo}}{dz}$	i=5,6,7,8
$b_{i,i+8} = \dfrac{u_{zo}}{\bar{c}h_o}[u_{\theta o}f_{so}a + (u_{\theta o}-1)f_{so}b]$	i=5,6,7,8
$b_{i+6,i} = -b_{i+8,i-2} = P_c/\tilde{\rho}_o$	i=3,4
$b_{i+4,i} = \dfrac{1}{\bar{c}h_o\tilde{\rho}_o}[u_{\theta o}m_s f_{so} + (u_{\theta o}-1)m_r f_{ro}]$	i=5,6,7,8
$b_{i,i} = \dfrac{u_{zo}}{\bar{c}h_o}[u_{\theta o}f_{so}a + (u_{\theta o}-1)f_{ro}b] + \dfrac{1}{\ell}\dfrac{du_{\theta o}}{dz}$	i=9,10,11,12

$$b_{i,i+4} = \frac{1}{\bar{c}h_o}[f_{so}(1+u_{\theta o}{}^2 a)+f_{ro}(1+(u_{\theta o}-1)^2 b_1]$$

$i=9,10,11,12$

$$b_{i+12,i} = \frac{-\gamma u_{zo}}{\tilde{\rho}_o \ell}\frac{d\tilde{\rho}_o}{dz} \qquad i=1,2,3,4$$

$$b_{i+11,i} = -b_{i+12,i-1} = \frac{\gamma'\tilde{\Omega}}{\gamma} \qquad i=2,4$$

$$b_{i+10,i} = -b_{i+13,i-1} = \gamma' u_{\theta o} \qquad i=3,4$$

$$b_{i+8,i} = \frac{\gamma' u_{zo}}{\ell\tilde{\rho}_o}\left(\frac{2\tilde{p}_o}{\tilde{\rho}_o}\frac{d\tilde{\rho}_o}{dz} - \frac{d\tilde{p}_o}{dz}\right) + \frac{q(1+m_r)}{\tilde{\rho}_o}$$

$i=5,6,7,8$

$$b_{i+7,i} = -b_{i+8,i-1} = -\gamma'\frac{\tilde{p}_o\tilde{\Omega}}{\tilde{\rho}_o} \qquad i=6,8$$

$$b_{i+6,i} = -b_{i+9,i-1} = -\gamma'\frac{\tilde{p}_o u_{\theta o}}{\tilde{\rho}_o} \qquad i=7,8$$

$$b_{i+4,i} = \frac{\gamma'}{\ell}\left(\frac{d\tilde{p}_o}{dz} - \frac{\tilde{p}_o}{\tilde{\rho}_o}\frac{d\tilde{\rho}_o}{dz}\right) + \frac{2u_{zo}}{\ell}\frac{du_{zo}}{dz} + \frac{u_{\theta o}}{\ell}\frac{du_{\theta o}}{dz}$$

$$+ qf_{ro}u_{zo} \qquad i=9,10,11,12$$

$$b_{i+3,i} = -b_{i+4,i-1} = u_{zo}\tilde{\Omega} \qquad i=10,12$$

$$b_{i+2,i} = -b_{i+5,i-1} = u_{zo}u_{\theta o} \qquad i=11,12$$

$$b_{i,i+1} = -b_{i+1,i} = u_{\theta o}\tilde{\Omega} \qquad i=13,15$$

$$b_{i,i+2} = -b_{i+2,i} = u_{\theta o}{}^2 \qquad i=13,14$$

<u>Vectors $\underline{C}$ and $\underline{D}$</u>

$$c_1 = d_4 = \frac{1}{\ell h_o}\frac{d(\tilde{\rho}_o u_{zo})}{dz}$$

$$c_2 = -d_3 = -\tilde{\rho}_o\tilde{\Omega}/h_o$$

$$c_3 = -d_2 = -\tilde{\rho}_o u_{zo}/h_o$$

$$c_5 = d_7 = \frac{u_{zo}}{ch_o{}^2}\,[(m_s-1)f_{so}+(m_r-1)f_{ro}]$$

$$c_9 = d_{12} = \frac{1}{\bar{c}h_o{}^2}\,[u_{\theta o}(m_s-1)f_{so}+(u_{\theta o}-1)(m_r-1)f_{ro}]$$

$$c_{13} = d_{13} = \frac{q(m_r-1)}{h_o}$$

$$c_{14} = -d_{15} = \frac{P_c\tilde{p}_o\tilde{\Omega}}{\tilde{\rho}_o h_o}$$